Original research

Patient-derived organoid biobank identifies epigenetic dysregulation of intestinal epithelial MHC-I as a novel mechanism in severe Crohn's Disease

Thomas W Dennison [1,2,3] Rachel D Edgar [4,5] Felicity Payne [1,2]
Komal M Nayak,[1,2] Alexander D. B. Ross,[1,2,6] Aurelie Cenier,[2,7] Claire Glemas,[1,8]
Federica Giachero,[1,2,8] April R Foster,[3,9] Rebecca Harris,[3] Judith Kraiczy,[2]
Camilla Salvestrini,[8] Georgia Stavrou,[2] Franco Torrente,[8] Kimberley Brook,[8]
Claire Trayers,[10] Rasa Elmentaite,[9] Gehad Youssef,[3] Bálint Tél [11]
Douglas James Winton,[1,12] Nefeli Skoufou-Papoutsaki,[1,12] Sam Adler,[1,12] Philip Bufler,[13]
Aline Azabdaftari,[13,14] Andreas Jenke,[15,16] Natasha G,[8] Natasha Thomas,[2]
Erasmo Miele [17] Abdulrahman Al-Mohammad,[2] Greta Guarda,[18]
Subra Kugathasan,[19,20] Suresh Venkateswaran,[19] Menna R Clatworthy,[21,22,23]
Tomas Castro-Dopico,[21] Ondrej Suchanek,[21,23] Caterina Strisciuglio,[24]
Marco Gasparetto,[25] Seokjun Lee,[1,3] Xingze Xu,[1,3] Erica Bello,[3] Namshik Han,[3,26]
Daniel R. Zerbino,[4] Sarah A Teichmann,[9,26,27] Josquin Nys,[28] Robert Heuschkel,[8]
Francesca Perrone,[1,2] Matthias Zilbauer [1,2,8]

Check for updates

ABSTRACT

Objective Epigenetic mechanisms, including DNA methylation (DNAm), have been proposed to play a key role in Crohn's disease (CD) pathogenesis. However, the specific cell types and pathways affected as well as their potential impact on disease phenotype and outcome remain unknown. We set out to investigate the role of intestinal epithelial DNAm in CD pathogenesis.

Design We generated 312 intestinal epithelial organoids (IEOs) from mucosal biopsies of 168 patients with CD (n=72), UC (n=23) and healthy controls (n=73). We performed genome-wide molecular profiling including DNAm, bulk as well as single-cell RNA sequencing. Organoids were subjected to gene editing and the functional consequences of DNAm changes evaluated using an organoid-lymphocyte coculture and a nucleotide-binding oligomerisation domain, leucine-rich repeat and CARD domain containing 5 (NLRC) dextran sulphate sodium (DSS) colitis knock-out mouse model.

Results We identified highly stable, CD-associated loss of DNAm at major histocompatibility complex (MHC) class 1 loci including *NLRC5* and cognate gene upregulation. Single-cell RNA sequencing of primary mucosal tissue and IEOs confirmed the role of NLRC5 as transcriptional transactivator in the intestinal epithelium. Increased mucosal MHC-I and NLRC5 expression in adult and paediatric patients with CD was validated in additional cohorts and the functional role of MHC-I highlighted by demonstrating a relative protection from DSS-mediated mucosal inflammation

in NLRC5-deficient mice. MHC-I DNAm in IEOs showed a significant correlation with CD disease phenotype and outcomes. Application of machine learning approaches enabled the development of a disease prognostic epigenetic molecular signature.

Conclusions Our study has identified epigenetically regulated intestinal epithelial MHC-I as a novel mechanism in CD pathogenesis.

WHAT IS ALREADY KNOWN ON THIS TOPIC

⇒ Epigenetics including DNA methylation may play a key role in the pathogenesis of Crohn's disease (CD). However, exact mechanisms remain ill defined.

WHAT THIS STUDY ADDS

⇒ Genome-wide molecular profiling as well as functional analyses of over 300 patient-derived intestinal organoids has identified epigenetically regulated major histocompatibility complex (MHC)-I as a novel mechanism in CD.

⇒ Our study demonstrates epigenetically regulated MHC-I function in the human intestinal epithelium suggesting a paradigm shift towards the intestinal epithelium as a non-classical antigen-presenting cell type.

⇒ Human gut organoids provide unique opportunities to investigate intestinal epithelial cell intrinsic mechanisms in CD making them ideal tools for drug testing and discovery.

HOW THIS STUDY MIGHT AFFECT RESEARCH, PRACTICE OR POLICY

⇒ Organoid-specific MHC-I DNA methylation correlates with clinical outcome highlighting the potential for the development of clinical biomarkers.

⇒ As organoids retain patient-specific epigenetic signatures, they can now be used for the development of novel drugs specifically targeting MHC-I.

INTRODUCTION

A hallmark of IBD, in particular Crohn's disease (CD), is the persistent chronic relapsing mucosal inflammation that favours specific gut segments such as the terminal ileum (TI).[1] Furthermore, despite successful resolution of mucosal inflammation in response to medical treatments, relapsing inflammation tends to recur in the same anatomical location. This phenomenon suggests the presence of stable molecular changes leading to altered function in local tissue-specific, resident cell types. Although altered function of the intestinal epithelium has been implicated in CD pathogenesis,[2 3] underlying mechanisms remain ill defined. One of the main obstacles to improving our understanding of intestinal epithelial cell (IEC)-specific mechanisms operative in human CD has been the lack of suitable, patient-derived experimental models. Human intestinal epithelial organoids (IEOs), which can be generated from mucosal stem cells and retain epigenetic signatures of host-derived tissues,[4–7] provide a novel opportunity to investigate the contribution of IEC intrinsic molecular mechanisms.[8] A major advantage of IEOs in the context of IBD is the ability to study IECs without exposure to their local inflammatory environment, thereby eliminating potentially confounding factors influencing gene expression and cellular function. As IEOs are derived from constantly dividing intestinal mucosal stem cells, disease-associated alterations that persist in culture would reflect IE cell-intrinsic and heritable pathologies. Thus, here we focused on DNA methylation (DNAm) as one of the main epigenetic modifications known to be operative in mammals that can cause heritable changes in cellular function in the absence of alterations to the DNA sequence.[9–12] DNAm is considered a highly stable epigenetic mark, which, once fully established, underpins lifelong tissue identity by regulating fundamental aspects of cellular function.[11 12] We and others have provided evidence for the important role of DNAm in regulating IEC function in vivo and in intestinal organoids.[13–15] Furthermore, altered DNAm has been linked to the pathogenesis of chronic, complex, multifactorial diseases including IBD.[9 16–19]

Here, we generated a living biobank of 312 IEO lines derived from mucosal biopsies of small (duodenum (DUO) and TI) and large bowel (sigmoid colon (SC)) of 168 patients diagnosed with CD (n=72), UC (n=23) and healthy controls (n=73). Genome-wide DNAm and transcriptional profiling of IEOs and matching primary intestinal epithelium was performed. In addition, the functional role of disease-associated DNAm changes was investigated using genetically modified human and murine IEOs, and a murine dextran sulphate sodium (DSS) colitis model. A range of computational approaches were used to identify CD-associated DNAm changes and their correlation to prospectively collected disease phenotype and outcomes.

MATERIALS AND METHODS

Patient recruitment, sample collection and clinical data recording

Patients were prospectively recruited at Cambridge University Hospitals, and biopsy samples obtained during diagnostic endoscopy. Diagnosis of CD and UC was made according to international guidelines.[20] Patients with normal macroscopic and histological appearance of their intestinal mucosa and complete resolution of any GI symptoms were classified as non-IBD, healthy controls. All patients were followed for a minimum of 18 months post diagnosis. Mucosal biopsies were obtained from DUO, TI and SC.

Patient and public involvement

Public and patient/parent engagement activities to inform our research included regular IBD family days as well as a bimonthly research newsletter and family events (see online supplemental file for further details).

Human IEO culture generation and biobank

IEOs were generated from intestinal crypts as previously described.[15 21] Following the expansion of IEOs over a minimum of 2 weeks in culture, frozen stocks were generated. Imaging was performed using an Incucyte and Opera Phoenix high-content imaging system (for further details, see online supplemental materials and methods).

Single-cell RNA sequencing

Single-cell RNA sequencing of IEOs and primary intestinal mucosal samples was performed using the 10× Genomics Chromium platform following dissociation into single cells as described previously.[22–24]

Clustered Regularly Interspaced Short Palindromic Repeats (CRISPR)- mediated gene editing of human IEOs

CRISPR-mediated KO for nucleotide-binding oligomerisation domain, leucine-rich repeat and CARD domain containing 5 (*NLRC5*) in IEOs was performed using a ribonucleoprotein-based method as described previously (online supplemental materials and methods).[25]

NLRC5-mCherry PiggyBac plasmid construct and IEOs transfection

The human *NLRC5* cDNA (*myc-NLRC5*) was obtained from AddGene (#37509). PiggyBac (PB)-*mCherry* transposon backbone plasmid, the PB transposase and rtTA-hygromycin resistance (rtTA-HygRes) plasmids were a generous gift from B.K. Koo (Institute for Basic Science, Korea). Transfection of IEOs, clonal selection and confirmation of successful overexpression were performed as described previously with minor modifications (online supplemental materials and methods).

Tissue freezing, sectioning and RNAscope

Human mucosal biopsies undergoing RNAscope analysis were processed and experiments were performed at the Cellular Generation and Phenotyping facility at the Wellcome Sanger Institute as described previously (online supplemental materials and methods).[24]

Mice

Mice were maintained at a Home Office-approved facility in the UK under specific pathogen-free conditions. *Nlrc5* floxed and

deficient mice (*Nlrc5$^{fl/fl}$* and *Nlrc5$^{-/-}$* mice on a C57BL/6 background) were donated by G. Guarda.[26] Spleens from OT-I Rag-deficient mice were donated by G. Griffiths. Colitis was induced using DSS, details provided as online supplemental file.

Murine IEO culture, organoid peptide stimulations and coculture with OTI T cells

Nlrc5$^{-/-}$ or *Nlrc5$^{fl/fl}$* mouse organoids were set up from two age and sex-matched mice per genotype, as previously described and used for cytokine stimulation as well as coculture experiments (online supplemental materials and methods).[27 28]

Data analyses
Publicly available datasets
Details for all publicly available datasets analysed are listed in online supplemental table S2.

DNAm and bulk RNA-seq data and analysis
Genome-wide DNAm was profiled using either the Illumina Infinium Human Methylation 450 BeadChip, or the Illumina EPIC platform.[29 30] DNAm data were processed as described previously with minor modifications. Further details on weighted gene coexpression network analysis (WGCNA), differential DNAm, pathway enrichment analyses and machine learning approaches to generate a prognostic and diagnostic DNAm signature as well as risk scores are provided in the online supplemental materials and methods. Bulk RNA-seq data were processed using standard computational approaches as described previously.[19] An average major histocompatibility complex class I (MHC-I) gene expression score comprising the genes *NLRC5*, *TAP1/2*, *PSMB8/9*, *HLA-A/-B/-C/-E/-F/-G*, *IRF1* and *B2M* was calculated, subtracted by the aggregated expression of 100 control gene sets (see online supplemental file).

Single-cell RNA-seq data analyses
Single-cell RNA-seq data were analysed as described previously using a number of software packages including CellRanger.[23 24] Details on scRNA-seq data analysis are provided as online supplemental materials and methods.

Statistical analysis
Statistical analysis was performed using GraphPad Prism software or R. Plots with CIs show mean±SEM unless otherwise indicated. For in vivo experiments, sample sizes were determined based on previous experiments.[31] For t-tests, assumptions of normality and equal variance were confirmed using the Shapiro-Wilk test and by confirming higher to lower SD ratios were below 2.

RESULTS
Molecular profiling of patient-derived IEOs reveals stable loss of MHC-I and *NLRC5* DNAm in the intestinal epithelium of patients with CD

We generated IEOs from 168 patients diagnosed with CD (n=73), UC (n=24) healthy controls (n=71, table 1 and online supplemental table S1). Following in vitro culture of organoids for 1–2 passages (average 2–3 weeks), genome-wide DNAm profiling was performed, and frozen organoid stocks stored in an organoid biobank (figure 1A, table 1 and online supplemental tables S1 and S2). Organoid growth, viability and structure were monitored over time with no major disease-associated differences observed on a microscopic level (figure 1Aii and online supplemental figure S1A). Next, to identify disease-associated DNAm changes that are retained in IEOs, we applied a WGCNA to TI organoid methylation. WGCNA enables unsupervised identification of highly correlated groups of CpGs (termed modules) as well as their correlation with phenotypes (ie, CD, UC, controls). As shown in figure 1B, analyses revealed several modules that significantly correlated with a diagnosis of CD with the most strongly correlated module (module 17, p <0.001) demonstrating a loss of DNAm in patients with CD (figure 1Bi). Gene ontology analyses preformed on genes containing CpGs forming module 17 showed significant enrichment scores for pathways related to '*antigen processing and presentation via MHC-I*'. Genes-encoding key components of MHC-I signalling include *PSMB8/9*, *HLA-B,-C and F*, *TAP1/2* and *B2M* (figure 1Bii and online supplemental figure S1B). Similar results were obtained when applying WGCNA analyses to IEOs derived from the SC (online supplemental figure S1C). Results were further confirmed by performing differential DNAm analyses, identifying a total of 234 hypomethylated CpGs in both TI and SC organoids derived from patients with CD that were found to be enriched for MHC-I related pathways (online supplemental figure S1D). Importantly, among the most significant loci showing loss of DNAm in patients with CD were two CpGs located within the promoter region of *NLRC5* (cg07839457 and cg07862320), a known transcriptional regulator/transactivator of MHC-I[32 33] (figure 1C and online supplemental figure S1E).

Average DNAm loss of *NLRC5* and MHC-I related genes in CD compared with control organoids was found to reach 20% in both TI and SC, while no differences were observed in the

---

Table 1 Patients and intestinal organoids

Patients				Organoid lines			
Diagnosis	**Number**	**Gender Female/male**	**Age at diagnostic endoscopy (average±SD)**	**Gut segment**	**Number**	**Inflamed versus non-inflamed**	**Culture duration (average passage no ±SD)**
Controls	71	41/30	9.77±4.24	Duodenum	20	0/20	2.55 (SD=2.31)
				Terminal ileum	57	0/57	3.33 (SD=3.51)
				Sigmoid colon	52	0/52	2.73 (SD=1.55)
UC	24	16/8	10.62±3.59	Duodenum	8	0/8	2.63 (SD=1.60)
				Terminal ileum	16	0/16	2.81 (SD=1.38)
				Sigmoid colon	18	16/2	2.33 (SD=1.19)
Crohn's disease	73	29/44	12.61±2.42	Duodenum	26	8/18	1.65 (SD=0.75)
				Terminal ileum	56	37/19	2.50 (SD=2.30)
				Sigmoid colon	61	49/12	2.30 (SD=1.58)
Total	168				314		

Figure 1 Stable loss of major histocompatibility complex class I (MHC-I) gene DNA methylation (DNAm) in intestinal epithelial organoids (IEOs) derived from patients with Crohn's disease (CD). (A) (i) Overview of experimental set-up and sample generation. (ii) Representative brightfield images of IEOs. Scale bars: 300 μm. (B) (i) Correlation heat map of comethylated CpG modules identified by weighted gene coexpression network analysis (WGCNA) in terminal ileum (TI) IEOs. Module 17 (ME17) demonstrates hypomethylation and the strongest association with CD diagnosis (R=−0.43, p value<0.001). (ii) Gene set enrichment analysis performed on module 17, showing a significant loss of DNAm in CD organoids compared with healthy controls and UC in TI. (C) DNAm (beta value) of four representative MHC-I related Differential Methylated Positions (DMPs) showing CD-associated loss of DNAm in TI and sigmoid colon (SC) but not duodenum (DUO) organoids (DUO=54, TI=127 and SC=131). (D) Average DNAm (beta value) of all CpGs located in MHC-I related genes for IEOs split by diagnosis, gut segment and inflammatory status. (E) (i) Correlation of nucleotide-binding oligomerisation domain, leucine-rich repeat and CARD domain containing 5 (NLRC5) promoter DNAm between early and later passage IEOs from the same individuals including patients diagnosed with CD (blue), UC (yellow) and controls (grey, n=22 patients. (ii) DNAm (beta values) of CpGs located in NLRC5 and TAP1 at high passage (>7) IEOs (cohort 1, n=22). (F) Average MHC-I (i) and NLRC5 (ii) DNAm as well as NLRC5 gene expression (iii) in control patient-derived TI IEOs stimulated with proinflammatory cytokines interferon γ (IFNγ) and tumour necrosis factor α (TNFα) (n=5). (False Discovery Rate (FDR) * < 0.05, FDR **< 0.01, FDR***< 0.001, FDR****< 0.0001, ns=not significant.)

DUO (figure 1C and online supplemental figure S1E,F). To investigate IE MHC-I DNAm more broadly, we computed a summary methylation score by calculating average DNAm levels of all CpGs associated with genes known to be involved in the MHC-I pathway (see the Methods section). Interestingly, intestinal epithelial MHC-I DNAm shows distinct regional variation in healthy individuals with the lowest levels observed in the TI (figure 1Di). Furthermore, as shown in figure 1Dii, global loss of MHC-I DNAm was observed in IEOs derived from patients with CD compared with healthy controls in both the TI and SC, but not in the DUO. Loss of MHC-I DNAm was also observed in the SC of patients with UC compared with controls, although not reaching statistical significance. Importantly, CD-specific loss of DNAm is, at least in part, independent of the presence of mucosal inflammation. Specifically, as shown in figure 1Diii, lower MHC-I DNAm was also observed in IEOs derived from non-inflamed TI mucosal biopsies obtained from patients with CD. In contrast, no significant loss of MHC-I DNAm was observed in DUO organoids derived from patients with CD despite the presence of mucosal inflammation (figure 1Div). The fact that disease-associated MHC-I DNAm changes are retained in IEOs following multiple passages/cell divisions indicates a high degree of stability, as well as mitotic heritability. Indeed, we found that CD-associated DNAm changes remained stable even when cultured in vitro over prolonged periods (ie, over several months) and in the absence of inflammatory stimuli. As shown in figure 1Ei, *NLRC5* DNAm was highly correlated in organoids profiled in early (1–6 passages) versus late (>6 passages) IEOs and CD-associated loss of *NLRC5* and *TAP1* DNAm retained in late passage IEOs (figure 1Eii and online supplemental figure S1G). Furthermore, stimulation of IEOs with IBD relevant inflammatory cytokines IFNγ and tumour necrosis factor α (TNFα), while inducing strong transcriptional changes, did not alter MHC-I DNAm (figure 1F, online supplemental figure S2A,B), further highlighting the stability of these epigenetic marks and their independence of the inflammatory milieu.

Taken together, these findings suggested stable loss of DNAm in MHC-I pathway genes, including the promoter region of *NLRC5* in the intestinal epithelium of patients with CD.

CD-associated loss of intestinal epithelial DNAm in MHC-I is associated with increased gene transcription in vivo and in vitro

Next, we analysed genome-wide DNAm and transcriptional profiles of primary IE obtained from patients newly diagnosed with CD, UC and healthy controls (cohort 2, figure 2A, online supplemental table S2).[19] Results confirmed CD-associated global loss of MHC-I DNAm and at individual CpGs including *NLRC5* in both TI and SC epithelium (figure 2Bi,Ci, online supplemental figure S3Ai). A significant loss of MHC-I DNAm was also observed in the SC epithelium of patients with UC, although to a lesser extent than CD (figure 2Ci). To survey broad intestinal epithelial MHC-I transcription, we calculated a global MHC-I expression score (supplementary methods). We found a highly significant inverse correlation between MHC-I DNAm and gene expression in TI and SC epithelium (figure 2Bii,Cii, online supplemental figure S3Aii,B). Next, we tested the stability of IE MHC-I DNAm in vivo by analysing primary IEC DNAm obtained from patients with IBD at diagnosis and several months after the initiation of treatment.[28] Consistent with findings in IEOs, CD-associated epigenetic changes including loss of *NLRC5* promoter DNAm were also stable in patients after several months of treatment (figure 2D). Consistent with these findings, we

observed a highly significant correlation between genome-wide IEC DNAm at diagnosis and repeat assessment (figure 2E and online supplemental figure S3C). Lastly, to confirm the impact of disease-associated loss of MHC-I DNAm on gene transcription in vitro, we compared *NLRC5* expression levels in IEOs derived from patients with CD with UC and healthy controls. As shown (figure 2F,G), IEOs derived from patients with CD harbouring lower *NLRC5* promoter DNAm had significantly higher *NLRC5* expression levels compared with UC and non-IBD controls (online supplemental figure S3D). Importantly, lower *NLRC5* promoter DNAm levels in patients with CD was also found to be associated with a higher level of gene expression in response to IFNγ compared with organoids derived from control patients (figure 2G).

These findings validated stable loss of MHC-I and *NLRC5* DNAm in primary epithelium of patients with CD as well as showing cognate gene upregulation.

NLRC5 functions as transcriptional transactivator for MHC-I in the intestinal epithelium and augments the effect of IFNγ

We next investigated *NLRC5*-dependent regulatory mechanisms in the context of inflammation. Applying CRISPR/Cas9 gene editing and the piggyBac transposon system to human IEOs, we generated *NLRC5* KO and inducible *NLRC5*-overexpressing organoids, respectively (figure 3A). Following stimulation with inflammatory cytokines IFNγ and TNFα, IEOs were subjected to transcriptional profiling (figure 3A). *NLRC5* overexpression resulted in significant upregulation of MHC-I genes to levels comparable to IFNγ-treated wild-type (WT) IEOs (figure 3B,C, online supplemental figure S4A). Flow cytometric analysis and immunostaining confirmed increased MHC-I protein expression on the surface of the IE (online supplemental figure S4B). Importantly, exposure of IEOs overexpressing *NLRC5* to IFNγ led to a further increase in MHC-I expression, suggesting an additive/potentiating effect of *NLRC5* on intestinal epithelial MHC-I (figure 3B,C). TNFα had little impact on MHC-I gene transcription (figure 3C, online supplemental figure S4A). In contrast, the treatment of human *NLRC5* KO IEOs with IFNγ led to reduced induction mRNA and protein levels of MHC-I genes compared with the WT IEOs (figure 3D,Ei,ii and online supplemental figure S4C). Pathway enrichment analyses performed on *NLRC5*-inducible genes confirmed a highly significant enrichment score for '*Antigen processing and presentation of peptide antigen via MHC-I*' (online supplemental figure S4D). Above results were confirmed in organoids derived from NLRC5-deficient mice (Methods, online supplemental figure S5). Lastly, in keeping with the in vitro results, *NLRC5* expression in primary purified IE from patients with CD, UC and control correlated significantly with expression of individual MHC-I genes (figure 3F, online supplemental figure S6).

Taken together, results demonstrate that *NLRC5* upregulates intestinal epithelial MHC-I and is capable of potentiating the effect of IFNγ.

Increased intestinal epithelial MHC-I expression in patients with CD affects the stem cell compartment

To gain further insight into the cell type-specific dynamics of MHC-I expression within IBD IE subsets, we performed single-cell RNA sequencing (scRNA-seq) on small bowel biopsies obtained from patients with IBD and controls (cohort 3, figure 4A, online supplemental table S2).[24] Major differences in MHC-I expression levels were observed between IEC subsets that correlated with their location along the crypt-villus axis
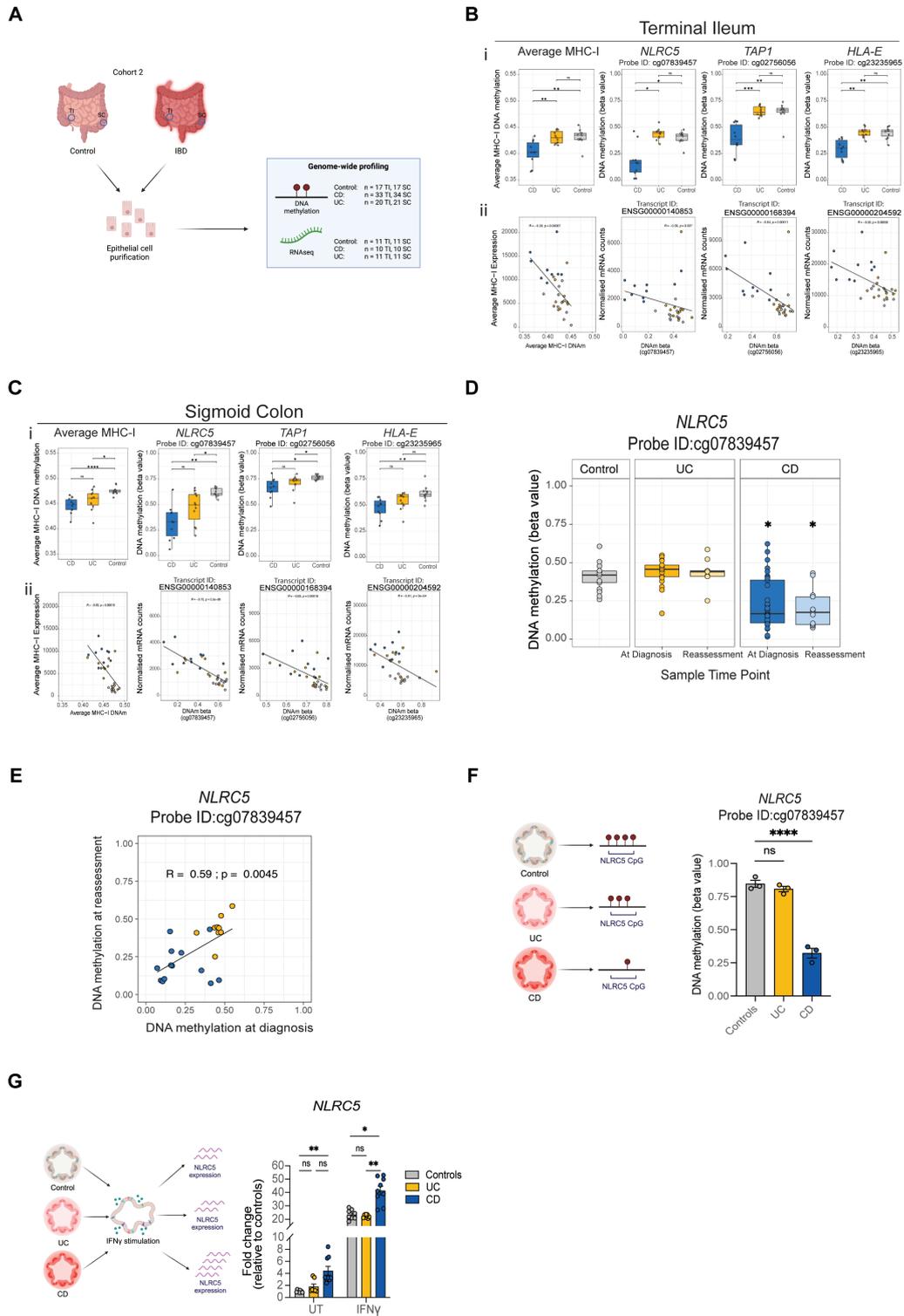
Figure 2 Loss of major histocompatibility complex class I (MHC-I) DNA methylation (DNAm) correlates with increased gene expression in primary intestinal epithelium of patients with Crohn's disease (CD). (A) Overview of patient cohort, sample preparation and data generation. (B, C) DNAm and gene expression in purified terminal ileum (TI) (B) and sigmoid colon (SC) (C) epithelium. (i) Average DNAm (beta value) of all and selected MHC-I pathway-related CpGs showing significant, CD-associated loss of DNAm. (ii) Correlation between beta values and corresponding gene expression (R=Spearman's rank correlation). (D) Nucleotide-binding oligomerisation domain, leucine-rich repeat and CARD domain containing 5 (*NLRC5*) promoter DNAm in the IE of healthy, patients with UC and CD at the point of diagnosis and during reassessment. (E) Correlation of *NLRC5* promoter DNAm in intestinal epithelial organoids (IEOs) obtained from the same patient at diagnosis and reassessment (Spearman's rank correlation). (F) *NLRC5* promoter DNAm in TI IEOs derived from patients with CD, UC and control (n=3 IEO per condition, two-way analysis of variance (ANOVA) with Turkey's test for multiple comparisons. ****p<0.0001). (G) *NLRC5* mRNA expression in TI IEOs derived from patients with controls, UC and CD at baseline and on interferon γ (IFNγ) treatment (10 ng/mL for 6 hours). Data are normalised to the mean of control lines and shown as mean±SEM (two-way ANOVA with Turkey's test for multiple comparisons. **P<0.01, *p<0.05, ns=not significant). n=3 IEO lines in each group for three independent experiments.
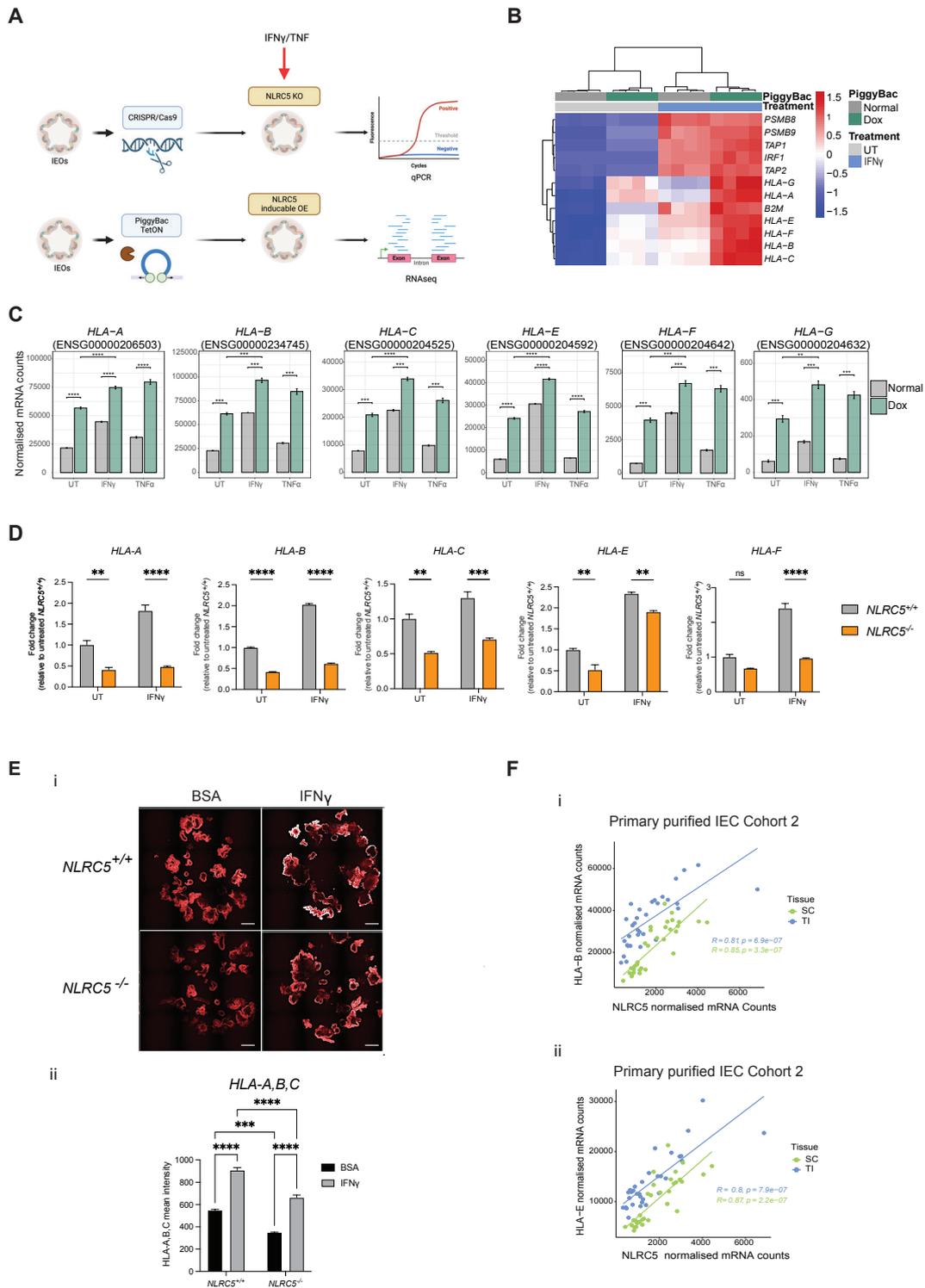
Figure 3 Nucleotide-binding oligomerisation domain, leucine-rich repeat and CARD domain containing 5 (*NLRC5*) acts as transcriptional transactivator of intestinal epithelial cell (IEC) major histocompatibility complex class I (MHC-I) and potentiates the effect of interferon γ (IFNγ). (A) Overview of experimental set-up. (B) Heatmap showing gene expression (RNAseq) of MHC-I pathway genes in terminal ileum (TI) intestinal epithelial organoids (IEOs)±*NLRC5* overexpression (dox), and ±exposure to IFNγ (n=4 independent replicates). (C) RNA transcription of *HLA-A/-B/-C/-E/-F/-G* in response to IFNγ and tumour necrosis factor α (TNFα) in wild type (WT) and NLRC5[OE] TI IEOs. (D) Relative expression for MHC-I pathway genes in WT (*NLRC5^+/+^*) and corresponding *NLRC5* deficient (*NLRC5^−/−^*) TI IEOs±IFNγ (n=3 replicates. Two-way analysis of variance (ANOVA) with Bonferroni's test for multiple comparisons, **p<0.01, ***p<0.001, ****p<0.0001). Data are representative of two independent experiments. (E) Immunofluorescence spinning disc microscopy of organoids described in D, ±IFNγ (48 hours). (i) Representative images of untreated (BSA) and treated (IFNγ) WT (*NLRC5^+/+^*) and *NLRC5* deficient (*NLRC5^−/−^*) TI IEOs taken by Opera Phoenix. Scale bar=2 mm. (ii) HLA-A,B,C mean intensity quantification of BSA and IFNγ *NLRC5^+/+^* and *NLRC5^−/−^* TI IEOs. (n=3 independent replicates. Two-way ANOVA with Bonferroni multiple comparisons test, **p<0.01, ***p<0.001, ****p<0.0001.) (F) Correlation between mRNA gene expression of *NLRC5* and (i) *HLA-B* and (ii) *HLA-E*, in purified TI and sigmoid colon (SC) epithelium (cohort 2) (Spearman's rank correlation).
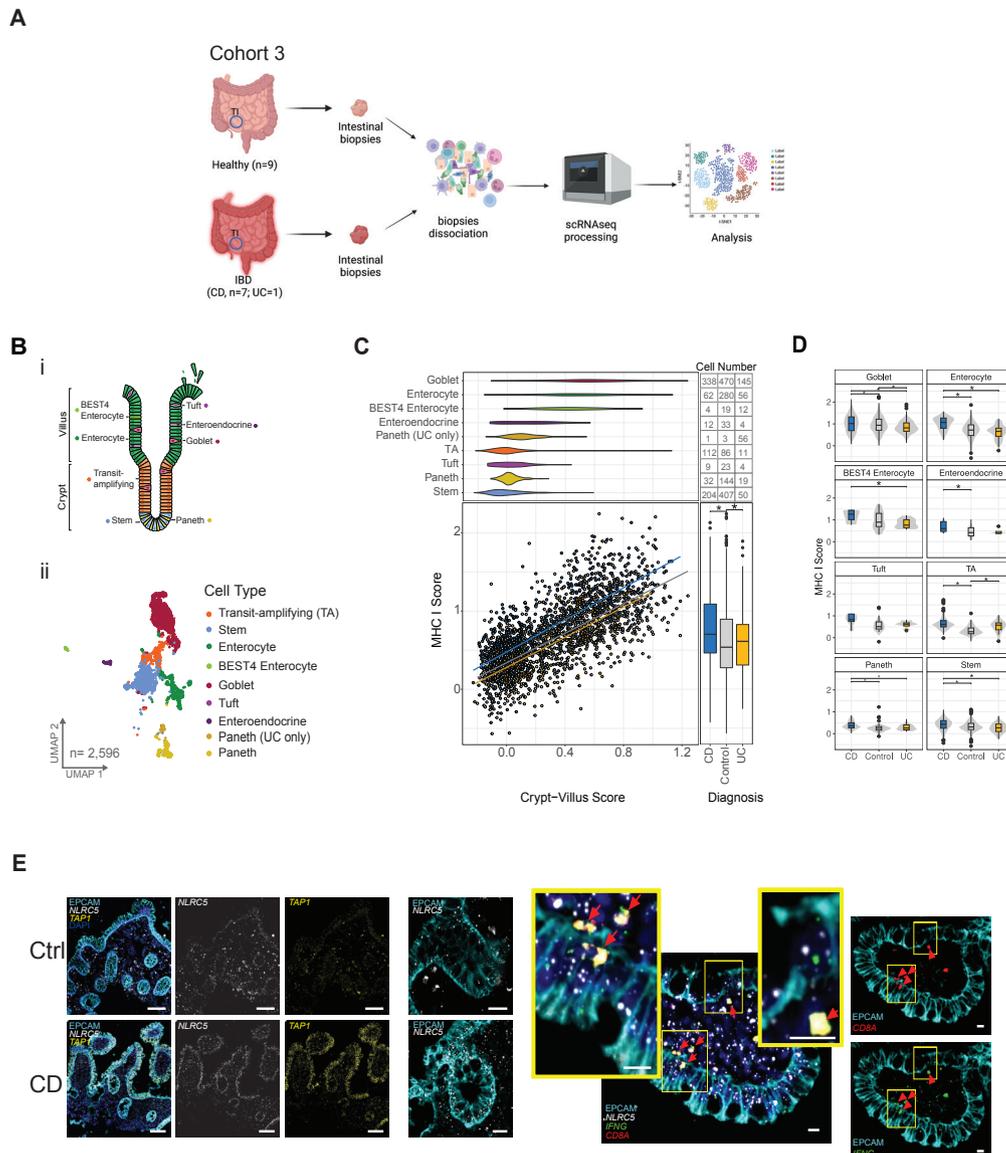
Figure 4 Crohn's disease (CD)-associated increased intestinal epithelial major histocompatibility complex class I (MHC-I) expression affects the stem cell compartment and follows a crypt-villus gradient. (A) Summary of experimental set-up. (B) (i) Schematic representation of intestinal epithelial cell (IEC) subtypes and their location within the small bowel (terminal ileum (TI)) crypt-villus structure (TA—transiently amplifying cells). (ii) Uniform manifold approximation and projection (UMAP) plot demonstrating single IEC transcriptomes present in TI mucosal biopsies obtained from children newly diagnosed with CD and non-IBD controls. (C) Top panel: violin plots showing crypt-villus scores of cells within each identified cell subtype (top left) and total number of cells (top right). Bottom panel: correlation between MHC-I summary score and crypt-villus scores for all IEC transcriptomes. Best fitting correlation is displayed as individual lines for CD (blue), UC (yellow) and non-IBD control samples (grey) (bottom left). Bottom right: box plots of summary MHC-I single-cell transcriptional score split by diagnosis. (D) Summary/average MHC-I score in individual IEC subtypes comparing CD, UC and controls. (E) Nucleotide-binding oligomerisation domain, leucine-rich repeat and CARD domain containing 5 (*NLRC5*) expression in TI IEC of patients with CD colocalises with CD8+ T cells. RNA scope of TI biopsies from healthy donors and patients with CD. *EPCAM* (cyan), *NLRC5* (white), *TAP1* (yellow), *CD8A* (red), *IFNG* (green) and nuclei (DAPI, blue). Proximity of CD8⁺ T-cells with NLRC5⁺EPCAM⁺ cells in the CD biopsy is shown with arrows. Representative images are shown. Scale bar=100 μm and zoom in scale bar=10 μm.

(figure 4B,C). Specifically, crypt-based epithelial stem cells, paneth cells and transiently amplifying cells demonstrated relatively low MHC-I expression levels compared with differentiated enterocytes located at the villus tip (figure 4C). Importantly, increased MHC-I expression levels were observed in TI epithelial cells of CD compared with healthy control and patients with UC (figure 4C, right lower panel). Moreover, increased expression reached statistical significance in most epithelial cell subsets including stem cells (figure 4D). This distinct crypt-villus gradient of IEC MHC-I expression was confirmed in the colonic epithelium of healthy individuals in two publicly available cohorts (cohort 4, online supplemental figure S7A,B, online supplemental table S2,[23] cohort 5, online supplemental figure S7C, online supplemental table S2).[34] Additionally, performing scRNAseq on IEOs stimulated with IFNγ confirmed a strong induction of MHC-I in all epithelial cell subsets and a crypt-villus expression gradient (online supplemental figure S7D–F). Lastly, RNAscope performed on TI biopsies further confirmed increased expression of *NLRC5* and *TAP1* in the intestinal epithelium of patients with CD and colocalisation with CD8+ T cells, indicating an epithelial cell-lymphocyte cross-talk via MHC-I (figure 4E).

These results indicated distinct MHC-I expression patterns in the IE along the crypt-villus axis with increased levels in the CD epithelium affecting the stem cell compartment.

Intestinal epithelial MHC-I can activate CD8+ T-cells and contribute towards mucosal inflammation in vivo and in vitro

Although all nucleated cells are considered as being capable of expressing MHC-I, limited information is currently available on the ability of the intestinal epithelium to present antigens and activate immune cells such as mucosal lymphocytes. To determine functional consequences of intestinal epithelial MHC-I in vitro and in vivo, we generated small bowel organoids from WT and NLRC5-deficient mice. Following exposure to IFNγ, organoids were pulsed with ovalbumin (OVA257-264) K^b-binding peptide (SIINFEKL) presented via murine MHC-I molecule (H2K^b, figure 5A). Flow cytometric analysis showed increased surface staining for MHC-I—ovalbumin (H2K^b-SIINFEKL) in organoids pretreated with IFNγ, confirming the ability of IECs to present antigen via MHC-I. *NLRC5* deficiency led to a significant reduction in IEC MHC-I—SIINFEKL complex expression (figure 5B, online supplemental figure S8A). Next, we generated IEOs from the small intestine of OT-I T-cell receptor transgenic mice. T-cells from these mice recognise ovalbumin peptides when presented by classical MHC-I (H2K^b). Coculture of IEOs with peptide-specific cytotoxic T-lymphocytes (CTLs) from OT-I mice led to their activation as indicated by increased IFNγ expression (figure 5C,D).

To investigate the role of NLRC5 in regulating intestinal MHC-I in vivo, we induced mucosal inflammation in WT and *NLRC5* deficient mice (figure 5E). Following exposure to DSS for 6 days, WT mice developed severe intestinal inflammation, resulting in up to 10% body weight loss at days 7–10. In contrast, NLRC5-deficient mice showed only mild symptoms and minimal weight loss (figure 5E). Reduced MHC-I expression on the surface of IECs in NLRC5 KO compared with WT mice was confirmed by flow cytometry (figure 5F, online supplemental figure S8B). Although at day 14 (8 days post exposure to DSS) the body weight of WT mice had recovered, analyses of intestinal tissue still revealed histological signs of ongoing small and large bowel inflammation in WT compared with NLRC5 KO mice (online supplemental figure S8E). Furthermore, we

observed increased size of mesenteric lymph nodes and gut weight (figure 5G, online supplemental figure S8E), as well as significantly increased infiltration with mucosal inflammatory cells (online supplemental figure S8C,D).

Taken together, these findings demonstrate the ability of IECs to present antigens via MHC-I and activate CTL in vitro, with NLRC5 involved in modulating mucosal MHC-I in the context of gut inflammation.

Increased mucosal MHC-I and NLRC5 expression in CD mucosa across several patient cohorts
Having demonstrated epigenetically mediated increase of MHC-I expression in the intestinal epithelium of patients with CD and a key role of *NLRC5* in orchestrating mucosal immune responses, we speculated that increased transcriptional activity should be detectable in whole intestinal mucosal biopsies. We therefore analysed mucosal MHC-I gene transcription in two publicly available cohorts of patients with IBD and compared transcriptional profiles of biopsies with those obtained from primary purified intestinal epithelium (cohorts 2, 6 and 7, figure 6, online supplemental figure S9 and online supplemental table S2).[19 35 36] A highly significant increase in MHC-I and *NLRC5* gene transcription levels was found in TI and SC biopsies of patients with CD compared with non-IBD healthy controls (figure 6, online supplemental figure S9A,B). Expression patterns of whole biopsy samples matched those identified in primary purified IECs including a CD-specific increase in MHC-I and *NLRC5* expression in the colonic mucosa compared with patients with UC despite showing lower average mucosal expression of levels of IFNγ (online supplemental figure S9C).

Together, these results further confirm the strong induction of MHC-I and *NLRC5* in the inflamed small and large bowel mucosa of patients with CD across multiple independent patient cohorts.

Intestinal epithelial MHC-I DNAm signatures stratify patients with CD and correlate with disease behaviour
Our findings so far have shown a stable loss of MHC-I and *NLRC5* DNAm in patients with CD, leading to increased gene transcription. Combined with the high degree of stability in vitro and in vivo, we speculate that epigenetic alterations that are present at diagnosis and remain stable throughout the course of disease may impact on long-term disease outcome, phenotype and severity. Consistent with this hypothesis, unsupervised hierarchical clustering based on MHC-I DNAm profiles resulted in the separation of patients into three distinct subgroups. Specifically, clusters of MHC-I DNA hypomethylation (MHC-I DNAm low) were enriched for patients with CD in both small (TI) and large bowel (SC) epithelium, while non-IBD/healthy controls represent the majority of samples within the MHC-I DNAm 'high' cluster (figure 7A and online supplemental figure S10A, right panels). A clear molecular stratification of patients with CD was also achieved based on unsupervised clustering of primary IEC or whole biopsy MHC-I gene expression profiles across multiple patient cohorts (online supplemental figure S11). Importantly, average MHC-I DNAm in TI organoids was found to differ significantly between patients with regards to several relevant disease phenotypes and outcome parameters including perianal disease, use of a thiopurine immunomodulator or biologics, as well as an overall more severe disease (based on a compound summary disease outcome/severity score, figure 7B and online supplemental figure S10B). Next, we aimed to develop a refined prognostic signature using combined WGCNA and machine
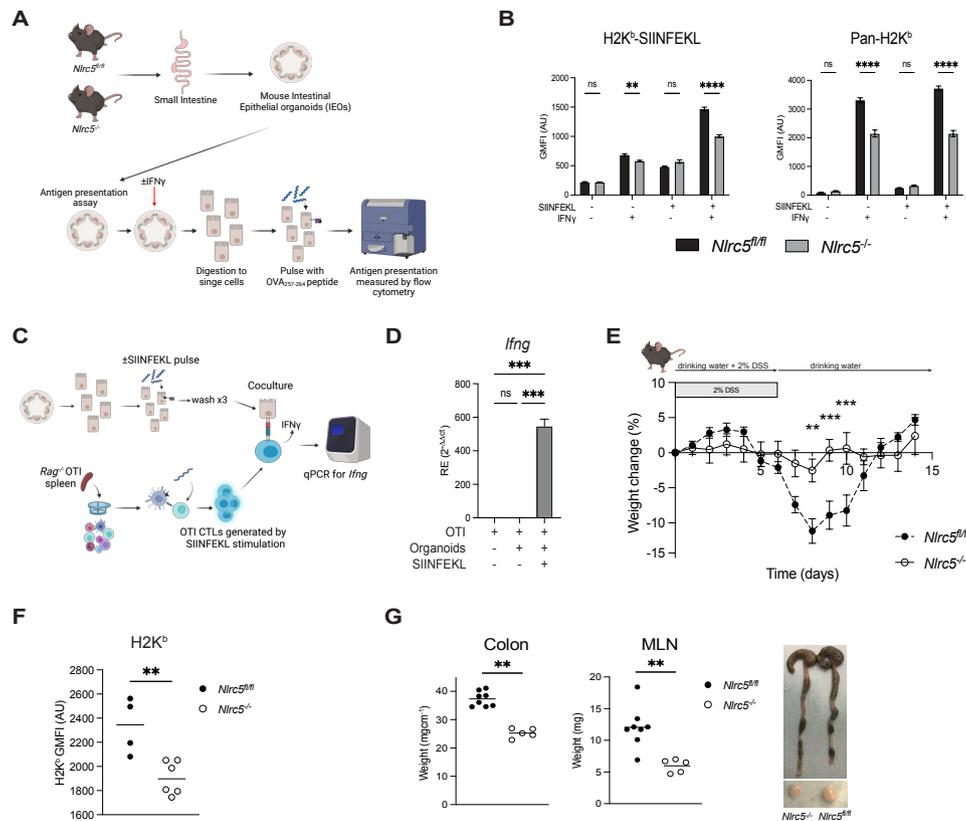
Figure 5 Intestinal epithelial cells (IECs) present antigen via major histocompatibility complex class I (MHC-I) and activate CD8$^+$ T cells in vitro with nucleotide-binding oligomerisation domain, leucine-rich repeat and CARD domain containing 5 (*NLRC5*) acting as key modulator of mucosal inflammation in vivo. (A) Overview of experimental set-up. (B) Quantification of H2K^b-SIINFEKL and pan-H2K^b flow cytometry on live EpCAM$^+$ cells in murine intestinal epithelial organoids (IEOs) stimulated with or without interferon γ (IFNγ) (48 hours) and pulsed with or without OVA257–264 peptide (SIINFEKL) peptide. Data are representative of two independent experiments run in triplicates. GMFI, geometric mean fluorescence intensity; AU, arbitrary units. P values were calculated by two-way analysis of variance (ANOVA) with Bonferroni test for multiple comparisons (**p<0.01, ****p<0.0001). (C) Overview of experimental design. (D) Quantitative PCR gene expression of *Ifng* for coculture experiment in murine IEOs±SIINFEKL peptide pulse and cocultured with SIINFEKL-activated OTI T-cells. Data are presented as fold change over unstimulated OTI cells minus murine IEOs, normalised to *Cd8a*. P values were calculated using two-way ANOVA with Bonferroni's multiple comparisons test (***p<0.001, ns=not significant). (E) Body weight changes over time during and after a 6-day course of 2% dextran sulphate sodium (DSS) exposure. (n=8 and n=5 *Nlrc5fl/fl* and *Nlrc5-/-* mice, respectively. P values calculated by multiple t-tests with Holm-Šídák correction for multiple comparisons.) (F) Quantification of H2K^b surface expression on EpCAM+ cell populations within the lamina propria extractions of DSS-treated mice. All panels: data are representative of two independent experiments (**p<0.01). (G) Colon weight per unit length and mesenteric lymph node (MLN) weight and spleen weight of *Nlrc5* wild type and knockout mice, on day 14 after initiation of 6-day course of 2% DSS (**p<0.01).

learning approaches (see the Methods section). As shown in figure 7C, results of analyses identified 28 MHC-I related CpGs (online supplemental tables S9 and S10) which allowed stratification of patients with CD into distinct molecular subgroups (figure 7Ci) and improved separation of patients with CD based on disease severity (figure 7Cii). Development of a risk score based on these 28 CpGs (see supplementary methods) allowed prediction of a severe disease outcome in patients with CD with receiver operator analyses returning 72% area under the curve (AUC 0.721, figure 7Ciii). Additionally, as shown in figure 7iv, using a cut-off risk score of >0.65 increases the prediction of a severe disease outcome from 43.6% to 72.7%, while in patients with a risk score <0.33, the posterior probability of a severe disease course drops to 18.2% (figure 7Civ). Lastly, applying the same computational strategies allowed identification of 53 MCH-I related CpGs that showed a high diagnostic accuracy for CD with an AUC of 0.82 (online supplemental figure S10C).

In summary, substantial variation in IEC MHC-I DNAm allows stratification of patients with CD into distinct molecular subgroups that correlate with disease phenotype and long-term outcome/disease severity.

DISCUSSION

Altered function of the intestinal epithelium has long been considered a key factor in CD pathogenesis. However, while major attention has been placed on potential mechanisms leading to impaired barrier function,[3 37 38] the potential role of the intestinal epithelium as an antigen-presenting and processing cell type has largely been neglected. Here, we have identified highly stable DNAm changes as the novel underlying mechanism leading to increased MHC-I expression in the intestinal epithelium of patients with CD. Generating adult stem cell-derived IEOs allowed us to eliminate the potentially confounding impact
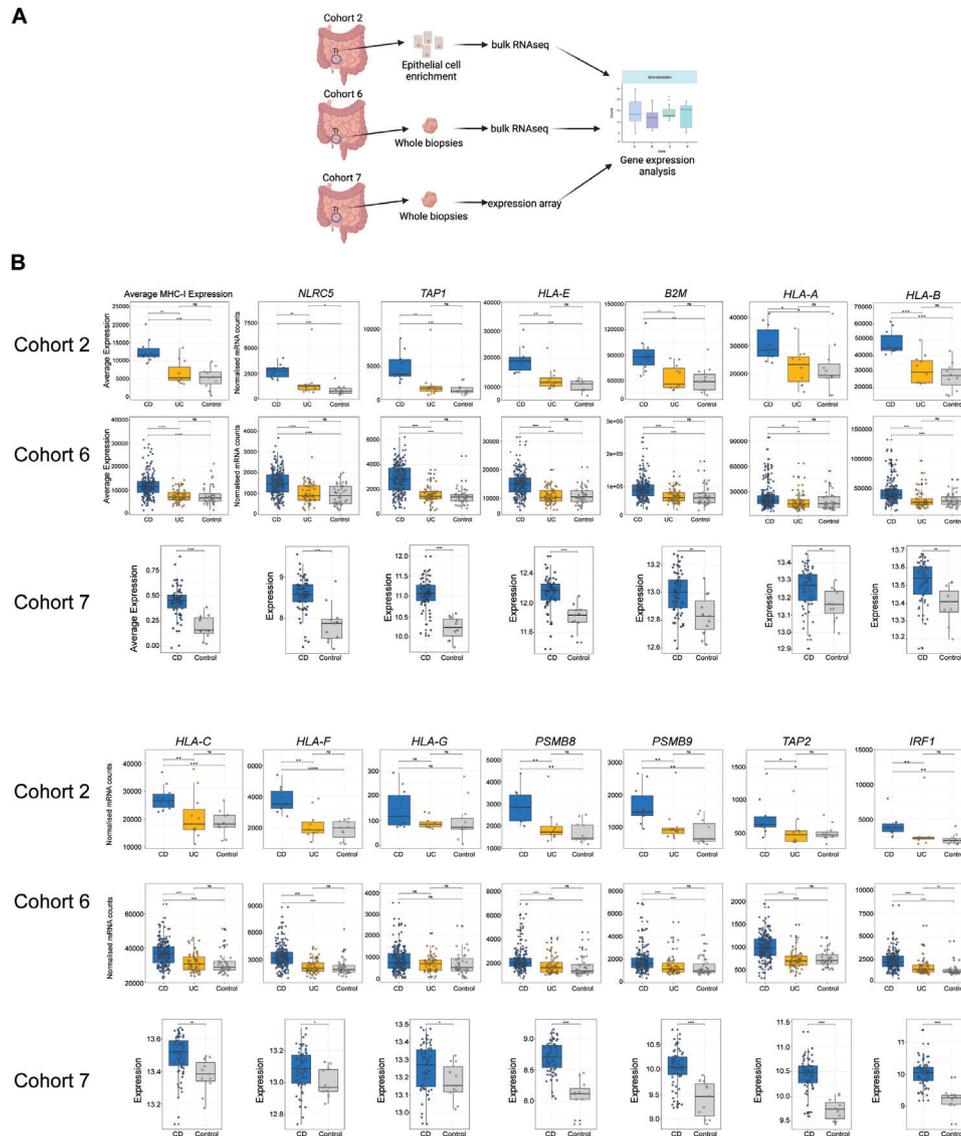
Figure 6 Increased major histocompatibility complex class I (MHC-I) gene expression in the small bowel intestinal mucosa of patients with Crohn's disease (CD) across different cohorts and data sets. (A) Overview of sampling sites and data types of cohorts 2, 6 and 7. (B) Average/summary MHC-I score and expression of selected MHC-I pathway genes. Expression split by diagnosis in TI biopsy samples from cohort 2 (n=32), cohort 6 (n=322) and cohort 7 (n=78).

of mucosal inflammation on DNAm as well as demonstrate the stability of DNAm in vitro. Specifically, given the fact that CD DNAm changes were retained in patient-derived IEOs and remained stable even over prolonged periods of in vitro culture indicates that epigenetic changes affect intestinal stem cells and are being inherited/passed on during mitosis in the absence of an inflammatory milieu. Our findings are in keeping with and provide mechanistic insight for previous studies reporting IBD-associated transcriptional differences in IEOs.[19 39–41] Furthermore, CD-associated DNAm changes observed in IEOs were validated in purified IECs and found to correlate with gene transcription (figure 2). Indeed, highly significant increased MHC-I gene expression was confirmed in mucosal biopsies from two large independent cohorts of adult and paediatric patients with CD.

Although the cause of stable DNAm changes in the intestinal epithelium of patients with CD remains speculative, our findings provide further evidence to support the emerging concept of inflammatory memory and trained innate immunity.[42 43]

Specifically, exposure to environmental triggers, occurring at critical periods during development, can lead to enduring epigenetic changes that determine cellular function. Together, with the continued exposure to an ever-wider range of new pathogens, pollutants and allergens, this mechanism has already been demonstrated in epithelial cells of the skin, lung and intestinal epithelium.[43–45] The well-known increase in incidence of IBD in countries such as India, China and the Middle East has been linked to the adoption of a more 'urban' lifestyle, highlighting the impact of recent changes in social environment on pathogenesis.[11]

Importantly, our study demonstrates that IEOs faithfully retain patient-specific, CD-associated DNAm changes in culture, further validating them as powerful translational research tools. Specifically, observed correlation between IEO-derived MHC-I DNAm signatures and disease severity highlights the major potential for these molecular signatures as clinical biomarkers. Larger validation studies are now underway to further enhance the value of cell-type intrinsic epigenetic signatures as clinical
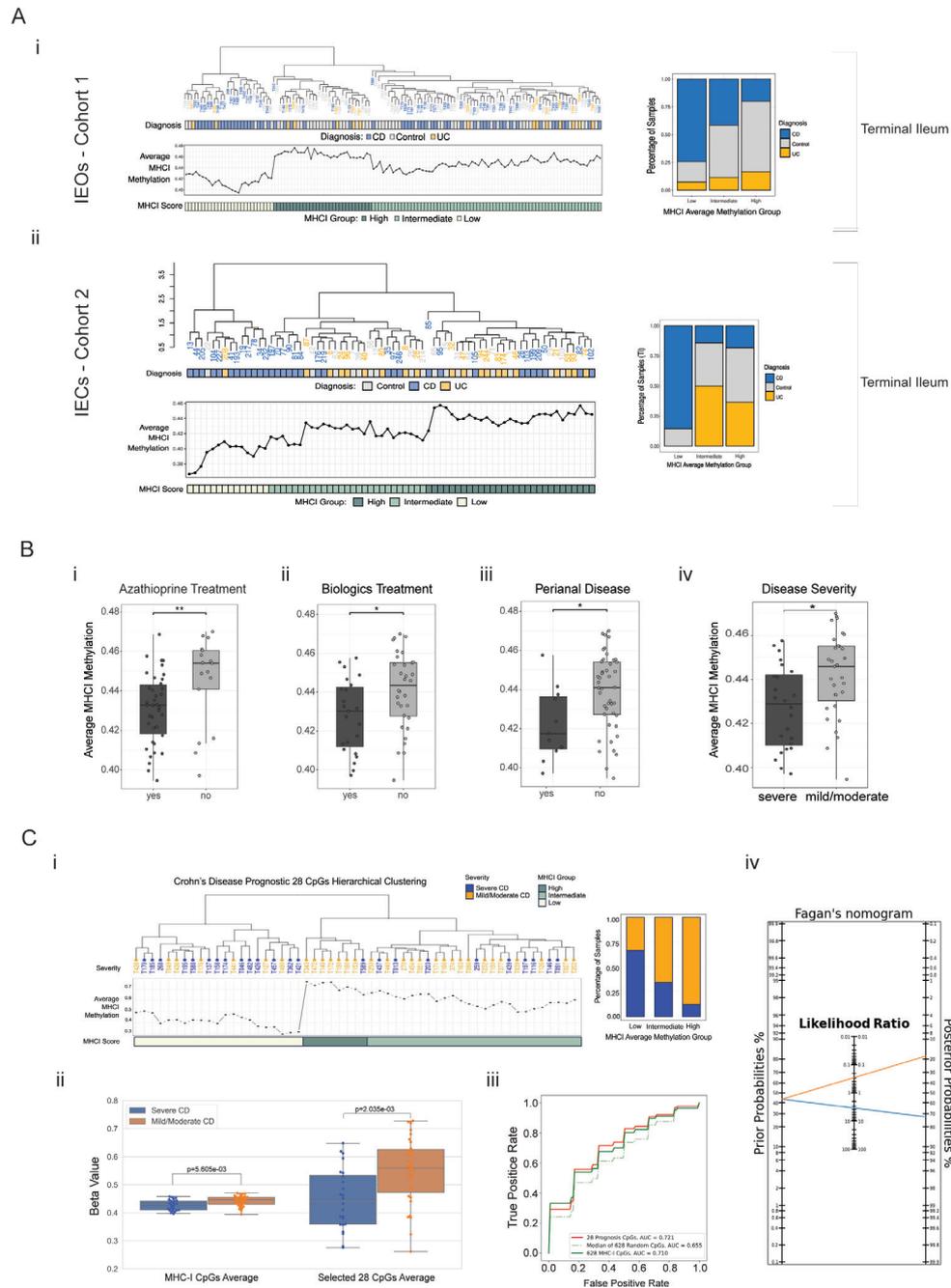
Figure 7 Intestinal epithelial cell (IEC) major histocompatibility complex class I (MHC-I) DNA methylation (DNAm) stratifies patients into distinct subgroups that correlate with phenotype and disease severity. (A) (i) Unsupervised hierarchical clustering of average MHC-I DNAm in terminal ileum (TI) (n=127) intestinal epithelial organoids (IEOs) (cohort 1). Distribution of IEOs based on the MHC-I DNAm score cluster is shown on the right. (ii) Unsupervised hierarchical clustering of average MHC-I DNAm in primary purified TI (n=70) IECs (cohort 2). Distribution of primary purified IECs based on the MHC-I DNAm score cluster split by diagnosis is shown on the right. (B) Average MHC-I DNAm score in TI IEOs derived from patients with Crohn's disease (CD) comparing disease outcome and phenotype: (i) patients with and without requirement for treatment with azathioprine; (ii) patients with and without treatment escalation to biologics; (iii) patients with and without the presence of perianal disease; (iv) patients with overall severe versus mild/moderate disease outcome. (C) (i) Unsupervised hierarchical clustering of average MHC-I DNAm in TI CD (n=55) IEOs (cohort 1). Distribution of IEOs based on the MHC-I DNAm score cluster split by disease severity is shown on the right. (ii) Box plot of average MHC-I DNAm and selected 28 prognostic CpGs in TI CD (n=55) IEOs (cohort 1), for CD samples with severe and mild/moderate disease outcomes, respectively. P values were calculated by two-way Welch's t-test (**p<0.01). (iii) Receiver Operating Characteristic Curve (ROC) curves and area under the curve (AUC) scores of logistic regression classifiers for CD severity prognosis using TI CD (n=55) IEOs (cohort 1), based on selected 28 prognostic CpGs, 628 MHC-I CpGs and median of random selections of 628 CpGs, respectively. (iv) Fagan's nomogram of CD severity risk stratification by prognostic risk scores (online supplemental figure S10C) based on selected 28 CpGs in TI CD (n=55) IEOs (cohort 1).

biomarkers. The availability of a large living organoid biobank, containing over 300 well-characterised lines, provides unique opportunities for the development of novel treatments specifically targeting intestinal epithelial MHC-I.

The current study does not go on to fully elucidate the complex downstream consequences of increased intestinal epithelial MHC-I expression and does not identify specific causative factors for the observed epigenetic changes. More work is required to fully understand the potential impacts of our observations.

Our study has identified epigenetically regulated intestinal epithelial MHC-I as a novel mechanism in CD pathogenesis. These findings support a paradigm shift towards the role of the intestinal epithelium as a non-classical antigen-presenting cell type directly driving chronic intestinal inflammation through increased interaction with mucosal lymphocytes.

Author affiliations
[1]Cambridge Stem Cell Institute, University of Cambridge, Cambridge, UK
[2]Department of Paediatrics, University of Cambridge, Cambridge, UK
[3]Milner Therapeutics Institute, University of Cambridge, Cambridge, UK
[4]European Bioinformatics Institute, Cambridge, UK
[5]Ajmera Transplant Centre, Toronto General Research Institute, University Health Network, Toronto, Ontario, Canada
[6]University Department of Medical Genetics, University of Cambridge, Cambridge, UK
[7]Technische Universität München, ZIEL – Institute for Food & Health, Freising, Germany
[8]Department of Paediatric Gastroenterology, Hepatology and Nutrition, Cambridge University Hospitals (CUH), Addenbrooke's, Cambridge, UK
[9]Wellcome Sanger Institute, Hinxton, UK
[10]Department of Paediatric and Perinatal Pathology, Cambridge University Hospitals (CUH), Addenbrooke's Hospital, Cambridge, UK
[11]Pediatric Center, MTA Center of Excellence, Semmelweis University, Budapest, Hungary
[12]Cancer Research-UK Cambridge Institute, Li Ka Shing Centre, Robinson Way, Cambridge, UK
[13]Department of Pediatric Gastroenterology, Nephrology and Metabolic Diseases, Charité-Universitätsmedizin Berlin, Corporate member of Freie Universität Berlin and Humboldt-Universität zu Berlin, Berlin, Germany
[14]Berlin Institute of Health (BIH) at Charité-Universitätsmedizin Berlin, Berlin, Germany
[15]Department of Neonatology and General Pediatrics, Children's Hospital Kassel, Kassel, Germany
[16]Clinical Molecular Genetics and Epigenetics, Centre for Biomedical Education and Research (ZBAF), HELIOS University Hospital Wuppertal, Witten/Herdecke University, Wuppertal, Germany
[17]Department of Translational Medical Science, Section of Pediatrics, University of Naples "Federico II", Naples, Italy
[18]Faculty of Biomedical Sciences, Institute for Research in Biomedicine (IRB), Università della Svizzera italiana, Bellinzona, Switzerland
[19]Department of Pediatrics, Emory University, Atlanta, GA, USA
[20]Department of Human Genetics, Emory University School of Medicine, Atlanta, GA, USA
[21]Molecular Immunity Unit, Department of Medicine, University of Cambridge, Cambridge, UK
[22]Cellular Genetics, Wellcome Sanger Institute, Hinxton, UK
[23]Cambridge Institute of Therapeutic Immunology and Infectious Diseases, University of Cambridge, Cambridge, UK
[24]Department of Woman, Child ad General and Specialistic Surgery, University of Campania " Vanvitelli", Naples, Italy
[25]Norfolk and Norwich University Hospital, Jenny Lind Children's Hospital, Norwich, UK
[26]Cambridge Centre for AI in Medicine, Department of Applied Mathematics and Theoretical Physics, University of Cambridge, Cambridge, UK
[27]Dept Physics/Cavendish Laboratory, Theory of Condensed Matter, JJ Thomson Ave, Cambridge, UK
[28]Bioscience Asthma and Skin Immunity, Research and Early Development, Respiratory & Immunology, BioPharmaceuticals R&D, AstraZeneca, Cambridge, UK

Competing interests None declared.

Patient consent for publication Not applicable.

Ethics approval This study involves human participants and was approved by REC 12/EE/0482 and REC 17/EE/0265. Participants gave informed consent to participate in the study before taking part.

Provenance and peer review Not commissioned; externally peer reviewed.

Data availability statement Data are available in a public, open access repository. Data are available upon reasonable request. All the information is provided in the main manuscript and online supplemental materials and methods. DNA Methylation data are available at ArrayExpress16 with Accession Numbers: E-MTAB-12841, E-MTAB-5463, Bulk RNA-seq data are available at ArrayExpress with Accession numbers: E-MTAB-5464., E-MTAB-11548. NLRC5-mCherry and mouse data are available on request. Single-cell RNA-seq data are available at ArrayExpress and SCP (singlecell.broadinstitute.org/single_cell) with Accession Numbers: E-MTAB-8901; SCP1884. All codes generated in this study are deposited and available on GitHub: https://github.com/ZilbauerLab/NLRC5_MHCI.Full dataset repository: https://www.ebi.ac.uk/biostudies/arrayexpress/studies/E-MTAB-12841?key=8aa7741a-673a-480f-a184-a73a7d9295b5

accuracy and reliability of the translations (including but not limited to local regulations, clinical guidelines, terminology, drug names and drug dosages), and is not responsible for any error and/or omissions arising from translation and adaptation or otherwise.

Open access This is an open access article distributed in accordance with the Creative Commons Attribution Non Commercial (CC BY-NC 4.0) license, which permits others to distribute, remix, adapt, build upon this work non-commercially, and license their derivative works on different terms, provided the original work is properly cited, appropriate credit is given, any changes made indicated, and the use is non-commercial. See: http://creativecommons.org/licenses/by-nc/4.0/.

ORCID iDs
Thomas W Dennison http://orcid.org/0000-0002-1449-7965
Rachel D Edgar http://orcid.org/0000-0001-5507-6078
Felicity Payne http://orcid.org/0000-0003-4228-581X
Bálint Tél http://orcid.org/0000-0003-2066-6494
Erasmo Miele http://orcid.org/0000-0003-4498-7305
Matthias Zilbauer http://orcid.org/0000-0002-7272-0547

REFERENCES

1 Torres J, Mehandru S, Colombel JF, et al. Crohn's disease. Lancet 2017;389:1741–55.
2 Strober W, Fuss I, Mannon P. The fundamental basis of inflammatory bowel disease. J Clin Invest 2007;117:514–21.
3 Kiesslich R, Duckworth CA, Moussata D, et al. Local barrier dysfunction identified by confocal laser endomicroscopy predicts relapse in inflammatory bowel disease. Gut 2012;61:1146–53.
4 Ungaro R, Mehandru S, Allen PB, et al. Ulcerative colitis. Lancet 2017;389:1756–70.
5 Dotti I, Salas A. Potential use of human stem cell-derived intestinal organoids to study inflammatory bowel diseases. Inflamm Bowel Dis 2018;24:2501–9.
6 In JG, Foulke-Abel J, Estes MK, et al. Human mini-guts: new insights into intestinal physiology and host-pathogen interactions. Nat Rev Gastroenterol Hepatol 2016;13:633–42.
7 Jung P, Sato T, Merlos-Suárez A, et al. Isolation and in vitro expansion of human colonic stem cells. Nat Med 2011;17:1225–7.
8 Kraiczy J, Zilbauer M. Intestinal epithelial organoids as tools to study epigenetics in gut health and disease. Stem Cells Int 2019;2019:7242415.
9 Dor Y, Cedar H. Principles of DNA methylation and their implications for biology and medicine. Lancet 2018;392:777–86.
10 Schübeler D. Function and information content of DNA methylation. Nature 2015;517:321–6.
11 Kaplan GG, Windsor JW. The four epidemiological stages in the global evolution of inflammatory bowel disease. Nat Rev Gastroenterol Hepatol 2021;18:56–66.
12 Straussman R, Nejman D, Roberts D, et al. Developmental programming of CpG Island methylation profiles in the human genome. Nat Struct Mol Biol 2009;16:564–71.
13 Sheaffer KL, Kim R, Aoki R, et al. DNA methylation is required for the control of stem cell differentiation in the small intestine. Genes Dev 2014;28:652–64.
14 Heppert JK, Davison JM, Kelly C, et al. Transcriptional programmes underlying cellular identity and microbial responsiveness in the intestinal epithelium. Nat Rev Gastroenterol Hepatol 2021;18:7–23.
15 Kraiczy J, Nayak KM, Howell KJ, et al. DNA methylation defines regional identity of human intestinal epithelial organoids and undergoes dynamic changes during development. Gut 2019;68:49–61.
16 Hodjat M, Rahmani S, Khan F, et al. Environmental toxicants, incidence of degenerative diseases, and therapies from the epigenetic point of view. Arch Toxicol 2017;91:2577–97.
17 Lorzadeh A, Romero-Wolf M, Goel A, et al. Epigenetic regulation of intestinal stem cells and disease: a balancing act of DNA and histone methylation. Gastroenterology 2021;160:2267–82.
18 Kellermayer R, Zilbauer M. The gut microbiome and the triple environmental hit concept of inflammatory bowel disease pathogenesis. J Pediatr Gastroenterol Nutr 2020;71:589–95.
19 Howell KJ, Kraiczy J, Nayak KM, et al. DNA methylation and transcription patterns in intestinal epithelial cells from pediatric patients with inflammatory bowel diseases differentiate disease subtypes and associate with outcome. Gastroenterology 2018;154:585–98.

20 Levine A, Koletzko S, Turner D, et al. ESPGHAN revised Porto criteria for the diagnosis of inflammatory bowel disease in children and adolescents. J Pediatr Gastroenterol Nutr 2014;58:795–806.
21 Edgar RD, Perrone F, Foster AR, et al. Culture-associated DNA methylation changes impact on cellular function of human intestinal organoids. Cell Mol Gastroenterol Hepatol 2022;14:1295–310.
22 Ross ADB, Perrone F, Elmentaite R, et al. Obtaining purified human intestinal epithelia for single-cell analysis and organoid culture. STAR Protoc 2021;2:100597.
23 Elmentaite R, Kumasaka N, Roberts K, et al. Cells of the human intestinal tract mapped across space and time. Nature 2021;597:250–5.
24 Elmentaite R, Ross ADB, Roberts K, et al. Single-cell sequencing of developing human gut reveals transcriptional links to childhood Crohn's disease. Dev Cell 2020;55:771–83.
25 Skoufou-Papoutsaki N, Adler S, D'Santos P, et al. Efficient genetic editing of human intestinal organoids using ribonucleoprotein-based CRISPR. Dis Model Mech 2023;16:dmm050279.
26 Staehli F, Ludigs K, Heinz LX, et al. Nlrc5 deficiency selectively impairs MHC class I-dependent lymphocyte killing by cytotoxic T cells. J Immunol 2012;188:3820–8.
27 Sato T, Vries RG, Snippert HJ, et al. Single Lgr5 stem cells build crypt-Villus structures in vitro without a Mesenchymal niche. Nature 2009;459:262–5.
28 Sato T, Stange DE, Ferrante M, et al. Long-term expansion of epithelial organoids from human colon, adenoma, adenocarcinoma, and Barrett's epithelium. Gastroenterology 2011;141:1762–72.
29 Pidsley R, Zotenko E, Peters TJ, et al. Critical evaluation of the Illumina Methylationepic BeadChip Microarray for whole-genome DNA methylation profiling. Genome Biol 2016;17:208.
30 Price ME, Cotton AM, Lam LL, et al. Additional annotation enhances potential for biologically-relevant analysis of the Illumina Infinium humanmethylation450 Beadchip array. Epigenetics Chromatin 2013;6:4.
31 Castro-Dopico T, Dennison TW, Ferdinand JR, et al. Anti-commensal IgG drives intestinal inflammation and type 17 immunity in ulcerative colitis. Immunity 2019;50:1099–114.
32 Kobayashi KS, van den Elsen PJ. NLRC5: a key regulator of MHC class I-dependent immune responses. Nat Rev Immunol 2012;12:813–20.
33 Neerincx A, Castro W, Guarda G, et al. NLRC5, at the heart of antigen presentation. Front Immunol 2013;4:397.
34 Kong L, Pokatayev V, Lefkovith A, et al. The landscape of immune dysregulation in Crohn's disease revealed through single-cell transcriptomic profiling in the ileum and colon. Immunity 2023;56:444–58.
35 Haberman Y, Tickle TL, Dexheimer PJ, et al. Pediatric Crohn disease patients exhibit specific Ileal transcriptome and microbiome signature. J Clin Invest 2014;124:3617–33.
36 Vancamelbeke M, Vanuytsel T, Farré R, et al. Genetic and transcriptomic bases of intestinal epithelial barrier dysfunction in inflammatory bowel disease. Inflamm Bowel Dis 2017;23:1718–29.
37 Nalle SC, Turner JR. Intestinal barrier loss as a critical pathogenic link between inflammatory bowel disease and graft-versus-host disease. Mucosal Immunol 2015;8:720–30.
38 König J, Wells J, Cani PD, et al. Human intestinal barrier function in health and disease. Clin Transl Gastroenterol 2016;7:e196.
39 Dotti I, Mora-Buch R, Ferrer-Picón E, et al. Alterations in the epithelial stem cell compartment could contribute to permanent changes in the mucosa of patients with ulcerative colitis. Gut 2017;66:2069–79.
40 Jelinsky SA, Derksen M, Bauman E, et al. Molecular and functional characterization of human intestinal organoids and monolayers for modeling epithelial barrier. Inflamm Bowel Dis 2023;29:195–206.
41 He S, Lei P, Kang W, et al. Stiffness restricts the stemness of the intestinal stem cells and Skews their differentiation towards goblet cells. Gastroenterology 2023;164:1137–51.
42 Naik S, Fuchs E. Inflammatory memory and tissue adaptation in sickness and in health. Nature 2022;607:249–55.
43 Larsen SB, Cowley CJ, Sajjath SM, et al. Establishment, maintenance, and recall of inflammatory memory. Cell Stem Cell 2021;28:1758–74.
44 Ordovas-Montanes J, Dwyer DF, Nyquist SK, et al. Allergic inflammatory memory in human respiratory epithelial progenitor cells. Nature 2018;560:649–54.
45 Naik S, Larsen SB, Gomez NC, et al. Inflammatory memory sensitizes skin epithelial stem cells to tissue damage. Nature 2017;550:475–80.